

# Fabrication of coupled quantum dots for multiport access

Alexander W. Holleitner and Robert H. Blick<sup>a)</sup>

*Sektion Physik and Center for Nanoscience, Ludwig-Maximilians-Universität, 80539 Munich, Germany*

Karl Eberl

*Max-Planck-Institut für Festkörperforschung, 70569 Stuttgart, Germany*

(Received 21 October 2002; accepted 27 January 2003)

We introduce a versatile two-step electron-beam fabrication technique for defining multiport quantum dots in GaAs/AlGaAs heterostructures in close vicinity. Capacitive coupling of the two quantum dots is directly tuned electrostatically via two central gates. Parallel access is realized by patterning source and drain contact regions of both dots with an additional spacer layer. Conductance measurements give evidence of both the continuous wide-range tunability of the dots and parallel access to the circuit. © 2003 American Institute of Physics.

[DOI: 10.1063/1.1563731]

Single electron effects such as Coulomb blockade were first detected on metal grains in 1951,<sup>1</sup> followed by corresponding measurements on superconducting particles in 1968.<sup>2</sup> Only in 1987 metal islands were lithographically defined<sup>3</sup> spurring experimental work on mesoscopic systems such as quantum point contacts<sup>4,5</sup> and quantum dots in GaAs/AlGaAs heterostructures.<sup>6</sup> Starting from Coulomb blockade in single quantum dots,<sup>7</sup> the combination of two capacitively coupled dots<sup>8</sup> allows us to investigate the electron-electron interaction in these few-electron systems. Recently, rather strong capacitive coupling was shown for lateral quantum dots by using a mediating metal film on the surface of the host semiconductor material, apparently increasing the capacitance between the two lateral quantum dots.<sup>9</sup> There, the dielectric and geometric constants of the interdot material determine the capacitance between the two quantum dots.

Here, we demonstrate a completely tunable method to vary the capacitance between two quantum dots in a wide range. In order to demonstrate this versatile method we utilize a bridging technique for Schottky gates, which was first used for parallel quantum point contacts<sup>10</sup> and recently introduced on quantum dots for establishing an Aharonov-Bohm interferometer containing two quantum dots.<sup>11,12</sup> The parallel access to both dots simultaneously even allows us to probe molecular states within the two quantum dots in a coherent fashion.<sup>13</sup>

The starting point for lateral quantum dots is a molecular-beam-epitaxy-grown GaAs/AlGaAs heterostructure (modulation doped) with a two-dimensional electron system (2DES), which in our case is located 90 nm beneath the surface. The mobility and sheet density of the 2DES are found to be  $80 \text{ m}^2/\text{Vs}$  and  $1.7 \times 10^{15} \text{ m}^{-2}$  at liquid-helium temperature. A Hall-bar-shaped mesa is defined using optical lithography and wet chemical etching. Furthermore, Ohmic contacts connecting the 2DES are provided by evaporated AuGeNi pads alloyed at 420 °C. Generally, quantum dots are defined by applying negative voltages to Schottky gates on top of the heterostructure and thus depleting the 2DES to quasi-zero-dimensional electron puddles with diameters of

about the Fermi wavelength  $\lambda_F \sim 50 \text{ nm}$ . These so-called split gates are defined on the Hall mesa using standard electron-beam lithography with subsequent metallization (3 nm of Ni/Cr and 30 nm of Au). For the purpose of contacting these split gates in the experiment, NiCr/Au bond pads are again patterned by optical lithography. All transport measurements are carried out in a  $^3\text{He}/^4\text{He}$  dilution refrigerator at the base temperature of 100 mK and a similar electron temperature in a standard lock-in technique.<sup>14</sup>

The central part of a typical sample is depicted by the atomic force microscope picture in Fig. 1(a). The areas of the 2DES providing two quantum dots are indicated by white dashed circles. Most notably, the source/drain contact regions of the dots are patterned with an additional 45-nm-thick spacer from negative resist Calixarene.<sup>15,16</sup> Gates 1 and 2 are constructed on top of these extra layers (white) finally forming a true quantum point contact (gray). Varying the voltages applied changes the distance between both dots and in turn, allows us to continuously tune the capacitive coupling of the dots in a wide range, as we will see below.

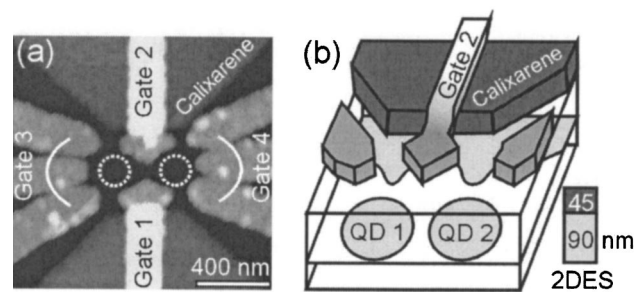


FIG. 1. (a) Atomic force micrograph and (b) schematic aerial view of two quantum dots which are defined in the two-dimensional electron system (2DES) of a GaAs/AlGaAs heterostructure. By evaporating gold gates on top of the heterostructure (gray) and applying negative voltages to these Schottky gates the two quantum dots are formed within the 2DES. In addition a dielectric spacer (dark gray) made from negative electron-beam resist Calixarene was deposited at the contact regions of the two quantum dots. The capacitive coupling can be tuned by varying the voltages on gates 1 and 2, which define both distance and capacitance between the two quantum dots. Individual source and drain ports of both dots are located beneath the upper and lower Calixarene layer.

<sup>a)</sup>Electronic mail: robert@nanomachines.com

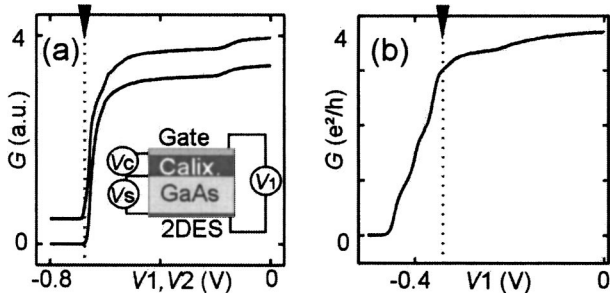


FIG. 2. Conductance–voltage characteristics of gates with (a) and without (b) the dielectric spacer underneath. Black triangles indicate the pinch-off voltages, respectively. Inset: schematic side view for pinch-off voltage in (a) with voltage drops across the Calixarene  $V_C$  and the semiconductor host material  $V_S$ .

Analogous to the tips of gates 1 and 2 the entire gates 3 and 4 are patterned directly on the surface of the heterostructure, which is 45 nm closer to the 2DES than the white areas of gates 1 and 2. In combination to the dielectric constant of Calixarene, this defines a range of gate voltages that on one hand depletes the 2DES beneath gates directly touching the surface of the heterostructure but on the other hand allows electrons to flow below the white parts of gates 1 and 2. This configuration allows parallel access to both quantum dots QD1 and QD2, as schematically depicted in Fig. 1(b).

Highlighting the shielding effect of the additional dielectric layer two conductance traces of gates—with and without Calixarene—are shown in Figs. 2(a) and 2(b) measured at zero bias voltage and  $T_{\text{bath}}=600$  mK. For bridged gates 1 and 2 we find pinch-off voltages of  $V_1,2 \sim -0.68$  V [see the triangle in Fig. 2(a)]. This voltage describes the pinch-off for electrons flowing in the 2DES below the Calixarene and the white parts of gates 1 and 2 in Fig. 1(a). For comparison, Fig. 2(b) depicts a typical conductance voltage characteristic for one of the quantum point contacts connecting the dots to source/drain. As expected for quantum point contacts, the conductance trace exhibits thermally broadened onsets of plateaus at  $e^2/h$  for voltages lower than  $V_S \sim -0.34$  V.

This voltage indicates the formation of one-dimensional channels within the quantum point contact,<sup>4,5</sup> and therefore, holds as a lower limit for the pinch-off voltage for gates without Calixarene beneath. The difference of both voltages describes the voltage drop via the Calixarene layer  $V_C \sim (V_{1,2} - V_S) = -0.34$  V. In addition, if we assume that the component of the displacement  $D_Z = \epsilon_0 \epsilon_r E_z$ , which is perpendicular to the 2DES is constant all over the resist layer and the substrate [ $\epsilon_0$  and  $\epsilon_r$  are the dielectric (relative) constants and  $E_z$  is the electric field in the corresponding direction] we can estimate the ratio of the voltage drops across the Calixarene  $V_C$  and the substrate  $V_S$  [ see the inset in Fig. 2(a)] by

$$\frac{V_C}{V_S} = \frac{z_C E_C}{z_S E_S} = \frac{z_C \epsilon_S}{z_S \epsilon_C}, \quad (1)$$

where  $z_C = 45$  nm is the thickness of the Calixarene and  $z_S = 90$  nm is the depth of the 2DES ( $\epsilon_{C,S}$  are the relative dielectric constants of Calixarene and the substrate). Evaluating Eq. (1) we find an estimate for the dielectric constant of Calixarene to be  $\epsilon_C = 7.1 \pm 0.5$ .

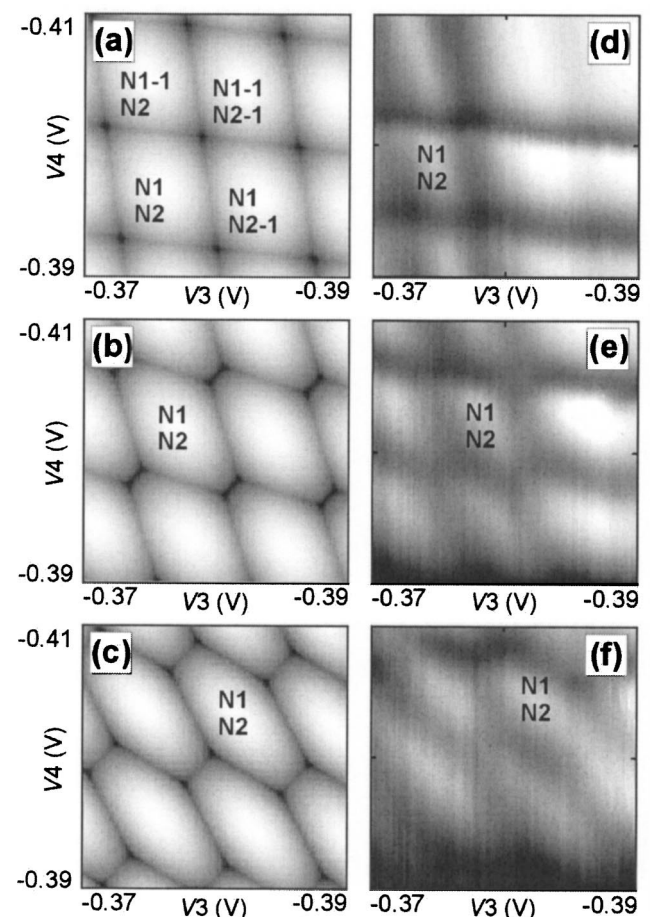


FIG. 3. (a)–(c) Simulated phase diagrams of a double quantum dot following Eq. (2) with an increasing interdot capacitance. Black indicates high electrostatic energy in arbitrary units. (d)–(f) Corresponding conductance measurement of a phase diagram of the double quantum dot in Fig. 1(a) (white  $\leq 0 \mu\text{S}$ , black  $\geq 4 \mu\text{S}$ ).

In the following we concentrate on the capacitive coupling of the two quantum dots. To this end, we model the electrostatic energy of the double quantum dot by the following biquadratic form:<sup>8,14</sup>

$$E_{\text{stat}} = \frac{1}{2} e \mathbf{N} \tilde{\mathbf{C}}^{-1} e \mathbf{N} - e \sum_{i=3,4,S,D,0} \boldsymbol{\alpha}_i \mathbf{N} V_i, \quad (2)$$

where  $\mathbf{N} = (N_1, N_2)$  describes the discrete number of electrons with charge  $e$  on quantum dot 1 and 2.  $V_i$  are voltages on different leads, namely, gates 3 and 4, the source/drain leads and a virtual gate “0” centralizing the sum effect of a background assumed to be constant. The model assumes that there is a specific capacitance between each gate and the particular dot. The capacitance themselves appear in  $\boldsymbol{\alpha}_i = (C_i/C_1, C_i/C_2)$  and translate the voltages applied to the gates into energy shifts on the dots with corresponding total capacitances  $C_1$  and  $C_2$ . The electrostatic electron–electron dot interactions are represented by the matrix  $\tilde{\mathbf{C}}$

$$\tilde{\mathbf{C}} = \begin{pmatrix} C_1 & C_{DD} \\ C_{DD} & C_2 \end{pmatrix},$$

with the interdot capacitance  $C_{DD}$  as the key element.

The effect of a varying interdot capacitance is displayed in the phase diagrams of Figs. 3(a)–3(c), which depict the

electrostatic energy with respect to  $V_3$  and  $V_4$ , numerically, (a)  $C_{DD}=0$  aF, (b)  $C_{DD}=-17$  aF, and (c)  $C_{DD}=-40$  aF.<sup>17</sup> For a realistic simulation the total dot capacitances are taken from transport spectroscopy on each individual dot, i.e.,  $C_1 \approx 83$  aF and  $C_2 \approx 88$  aF, which correspond to addition energies of about  $E_C^{\text{dot1}}=e^2/C_{\Sigma}^{\text{dot1}}=1.93$  meV and  $E_C^{\text{dot2}}=1.82$  meV. Hereby, we model the quantum dots as electronic disks with a capacitance  $C=8\epsilon_0\epsilon_r r_e$  ( $\epsilon_r \approx 12.8$  in GaAs),<sup>14</sup> which enables us to estimate the dot radii to be  $r_e \approx 90$  nm in good agreement with the lithographic dimensions seen in Fig. 1(a). Furthermore, by using the 2DES electron density we can assess the number of electrons in each dot to be less than 50.

Most importantly, the phase diagrams of Figs. 3(a)–3(c) yield information about the ground states of the double quantum dot with well-defined discrete numbers of electrons ( $N_1, N_2$ ) in reference to the experimental gate voltages  $V_3$  and  $V_4$ . Generally, along all phase boundaries the entire number of electrons can change by one enabling charge transport through the whole device. For parallel quantum dots this is verified in the following measurements: Figs. 3(d)–3(f) depict transport data on the double quantum dot from Fig. 1(a) for  $T_{\text{bath}}=100$  mK and zero dc bias. As expected, all experimental phase diagrams show conductance along all phase boundaries of the parallel double quantum dot. Furthermore, we were able to tune the capacitive coupling between the dots as predicted by Eq. (2) (see, also, Ref. 18).

In conclusion, we introduced two-step electron-beam lithography enabling the fabrication of two parallel quantum dots with individual source/drain contacts in a two-dimensional electron system of a GaAs/AlGaAs heterostructure. Cryogenic transport measurements prove functioning of the introduced spacer layer by shifting the pinch-off voltages for the Schottky gates in a wide range. Experimental phase diagrams demonstrate parallel connection of both dots while the capacitance between the two quantum dots can be tuned continuously.

The authors would like to thank J. P. Kotthaus for continuous support and stimulating discussions. The authors acknowledge financial support by the Deutsche Forschungsgemeinschaft through the Sonderforschungsbereich (SFB 348) and the Schwerpunkt “Quanteninformationsverarbeitung” (Bl/487-2-2), the Defense Advanced Research Projects Agency (EOARD Project No. F61775-01-WE037), and the Bundesministerium für Wissenschaft und Technik (BMBF Project No. 01BM914).

- <sup>1</sup>C. J. Gorter, *Physica (Amsterdam)* **17**, 777 (1951).
- <sup>2</sup>I. V. Giaever and H. R. Zeller, *Phys. Rev. Lett.* **20**, 1504 (1968).
- <sup>3</sup>T. A. Fulton and G. J. Dolan, *Phys. Rev. Lett.* **59**, 109 (1987).
- <sup>4</sup>D. A. Wharam, T. J. Thornton, R. Newbury, M. Pepper, H. Ahmed, J. E. F. Frost, D. G. Frost, D. G. Hasko, D. C. Peacock, D. A. Ritchie and G. A. C. Jones, *J. Phys. C* **21**, L209 (1988).
- <sup>5</sup>B. J. van Wees, H. van Houten, C. W. J. Beenakker, J. G. Williams, L. P. Kouwenhoven, D. van der Marel, and C. T. Foxon, *Phys. Rev. Lett.* **60**, 848 (1988).
- <sup>6</sup>U. Meirav, M. A. Kastner, and S. J. Wind, *Phys. Rev. Lett.* **65**, 771 (1990).
- <sup>7</sup>C. W. J. Beenakker, *Phys. Rev. B* **44**, 1646 (1991).
- <sup>8</sup>F. Hofmann, T. Heinzel, D. A. Wharam, and J. P. Kotthaus, *Phys. Rev. B* **51**, 13872 (1995).
- <sup>9</sup>I. H. Chan, R. M. Westervelt, K. D. Maranowski, and A. C. Gossard, *Appl. Phys. Lett.* **80**, 1818 (2002).
- <sup>10</sup>A. G. C. Haubrich, D. A. Wharam, H. Kriegelstein, S. Manus, A. Lorke, and J. P. Kotthaus, A. C. Gossard, *Appl. Phys. Lett.* **70**, 3251 (1997).
- <sup>11</sup>A. W. Holleitner, C. R. Decker, H. Qin, K. Eberl, and R. H. Blick, *Phys. Rev. Lett.* **87**, 256802 (2001).
- <sup>12</sup>A. W. Holleitner, R. H. Blick, H. Qin, A. K. Hüttel, K. Eberl, and J. P. Kotthaus, *Physica E (Amsterdam)* **12**, 774 (2002).
- <sup>13</sup>A. W. Holleitner, R. H. Blick, A. K. Hüttel, K. Eberl, and J. P. Kotthaus, *Science* **297**, 70 (2002).
- <sup>14</sup>L. P. Kouwenhoven, C. M. Marcus, P. L. McEuen, S. Tarucha, R. M. Westervelt, and N. S. Wingreen, in *Mesoscopic Electron Transport*, edited by L. L. Sohn, L. P. Kouwenhoven and G. Schön, NATO Advanced Study Institutes, Ser. E **345** (Kluwer, Dordrecht, 1997).
- <sup>15</sup>J. Fujita, Y. Ochiai, and S. Matsui, *Appl. Phys. Lett.* **68**, 1297 (1996).
- <sup>16</sup>A. Tilke, M. Vogel, F. Simmel, A. Krielle, R. H. Blick, H. Lorenz, D. A. Wharam, and J. P. Kotthaus, *J. Vac. Sci. Technol. B* **17**, 1594 (1999).
- <sup>17</sup>Capacitances between dot 1 (2) and gate 3 are taken to be  $C_{13}=-19$  aF ( $C_{23}=-2$  aF), respectively, gate 4:  $C_{14}=-3$  aF ( $C_{24}=-22$  aF).
- <sup>18</sup>U. Wilhelm and J. Weis, *Physica E (Amsterdam)* **6**, 668 (2000).